International Journal of Recent Technology and Engineering (IJRTE)
ISSN: 2277-3878 (Online), Volume-8 Issue-6, March 2020

Elastic and Elasto-Plastic Contact Behavior on Ball Bearing

Leong Chee Yau, Wan Fathul Hakim W. Zamri, Muhammad Faiz Md Din, Intan Fadhlina Mohamed, Azman Ahmad

Abstract: ***Contact pressure has a great influence on the realiability and the life of ball bearings. However, most of the previous contact and wear model mainly focussed on the elastic model. In this paper, considering the contact between ball bearing and inner ring, both elastic and elasto-plastic contact model are established to investigate the contact behaviour on ball bearing. Three types of materials have been used to compare the contact behaviour which are bearing steel, silicon nitride and aluminium oxide. Aluminium oxide experienced highest maximum contact pressure for elastic model while silicon nitride experienced highest maximum contact pressure for elasto-plastic model. The stress contour of elastic model was elliptical shape while elasto-plastic model was elliptical shape before the material yields.***

Keywords: ***Ball bearings, Contact, Elasto-plastic, Finite element method.***

I. INTRODUCTION

Damage to a ball bearing occurs when it has been operating for a particular period of time, and this damage is known as spalling of the rings and balls. Today, ball bearings have been optimized to deliver more power by reducing their dimensions. The contact surface area between the ball bearing components has been reduced, while the contact pressure has increased. A high contact pressure will lead to damage, such as spalling, in the ball bearings [11], [5], [18]. The cost of replacing a rolling bearing is $50.5 billion globally, and it will continue to rise over the next 10 years. Studies into the contact pressure on ball bearings will help the world to deal with various problems [2]. Ball bearings are subject to contact pressure in the inner and outer rings. Damage and spalling in ball bearings are difficult to predict accurately. In addition, the contact pressure and deformation on ball bearings cannot be determined experimentally. Theoretically, it is very difficult to accurately estimate the contact pressure, even though this method has been widely used in the past. An approximate model is usually used, such as in a contact analysis, to handle problems, but this method is not sufficiently accurate [12]. Finite element simulations can be used to determine the contact pressure and deformation of a ball bearing [19]. There are many materials other than bearing steel used in ball bearing. The most common material used is the bearing steel (GCr15). This is the most common hardened bearing steel that has high hardness and wear resistance. Therefore, it is widely used in automotive engine and other general machinery [16]. Besides, hybrid ball bearing that is made of ceramic material are brought into many applications since two decades ago [8]. Ceramic material like silicon nitride, zirconium dioxide and aluminium oxide perform with high efficiency in extreme condition like high loads, hot environment and high speed. The advantages of using ceramic are not only high wear resistance and high corrosion resistant but also low density, small thermal expansion coefficient and large elastic modulus. That is the reason that ceramic bearing is suitable to operate in extreme conditions and environment [4], [7], [15].

The related journal about elasto-plastic contact was studied by Kogut et al. 2002 [10]. The elasto-plastic contact simulation was carried out to study the deformable sphere and a rigid flat by using finite element method. The research done was only fundamental in contact for ball bearing because the contacting bodies are deformable in ball bearing whereas the flat in simulation was rigid. Moreover, the other journal by Nazir et al. 2018 [15] studied about the rolling contact fatigue of silicon nitride ball bearing. The three dimensional model was developed to study stress intensity factors in the ball bearing. The study focused on the interaction between the balls of the ball bearing. This research aimed to study how the surface cracks affect the rolling contact fatigue in silicon nitride ball bearing. The contact simulation between ball and ball was conducted by Kadam et al. 2018 [7] to study the contact stress in ball bearing made up of material of stainless steel, silicon nitride, zincronium oxide and aluminium oxide.

Manuscript received on February 10, 2020.
Revised Manuscript received on February 20, 2020.
Manuscript published on March 30, 2020.

* Correspondence Author

Leong Chee Yau*, Faculty of Engineering and Built Environment, Universiti Kebangsaan Malaysia, Bangi, Malaysia. Email: cheeyau_95@hotmail.com.

Wan Fathul Hakim W. Zamri*, Dept. of Mechanical and Manufacturing Engineering, Faculty of Engineering and Built Environment, Universiti Kebangsaan Malaysia, Bangi, Malaysia. Email: wfathul.hakim@ukm.edu.my.

Muhammad Faiz Md Din, Dept. of Mechanical and Manufacturing Engineering, Faculty of Engineering and Built Environment, Universiti Kebangsaan Malaysia, Bangi, Malaysia.

Intan Fadhlina Mohamed, Dept. of Mechanical and Manufacturing Engineering, Faculty of Engineering and Built Environment, Universiti Kebangsaan Malaysia, Bangi, Malaysia.

Azman Ahmad, Dept. of Mechanical and Manufacturing Engineering, Faculty of Engineering and Built Environment, Universiti Kebangsaan Malaysia, Bangi, Malaysia.

This research studied the contact simulation by using elastic model without considering the plasticity of material. Most the researches that have been conducted were only considering the elasticity of material except the simulation carried out by Raga et al. 2016 [17]. This research studied about the normal rolling contact of the silicon nitride rolling elements. The developed model was twin-disk tribometer but not the ball bearing model.

The researcher carried out a finite element simulation by using elasto-plastic model to study the stress of the silicon nitride material under different loading conditions.

This study was carried out using an elastic model and an elasto-plastic model for the ball bearing material of bearing steel, silicon nitride and aluminium oxide so as to consider both the elastic and plastic behaviour of the material. The objective of this study was to examine the stress distribution and the effects of elastic and elasto-plastic deformation on the contact analysis of ball bearings for different materials.

II. CONTACT MODEL OF BALL BEARING

When two or more bodies are loaded with a compressive load, the Hertzian theory can be applied and derived based on some assumptions which are the material of contacting bodies are homogenous and isotropic, the contact areas are relatively small compared with the radii of curvature of contacting solids, the stress and strain relationship of the material follows Hooke's law and the contacting surfaces are perfectly smooth [6], [9], [14]. The contact between a sphere and a plate was shown in Fig. 1. The sphere represents the ball of a ball bearing, while the plate represents the inner ring of the ball bearing. The inverse radius of curvature, R' of the contact model can be calculated by:

$$\frac{1}{R'} = \frac{1}{R_x} + \frac{1}{R_y} \tag{1}$$

where R_x is the radius of the sphere and the radius of the plate at the x-axis, and R_y is the radius of the sphere and the radius of the plate at the y-axis. The inverse Young's modulus, E' can be calculated by:

$$\frac{1}{E'} = \frac{1}{2}\left[\frac{1-v_A^2}{E_A} + \frac{1-v_B^2}{E_B}\right] \tag{2}$$

where v_A is Poisson's ratio for the ball, while v_B is the Poisson's ratio for the inner ring, and E_A and E_B are the Young's modulus for the material of the ball and inner ring, respectively. The dimensions of the contact area, for the ball and the inner ring are given by:

$$a = \left(\frac{3WR'}{E'}\right)^{\frac{1}{3}} \tag{3}$$

where W is the applied load. The maximum contact pressure can be calculated by using the dimensions of the contact area, a that were obtained from (3). The maximum contact pressure, P_{max} can be written as follows:

$$P_{\max} = \frac{3W}{2\pi a^2} \tag{4}$$

The maximum contact pressure on the ball bearing when a load is applied and the dimensions of the contact area are known can be calculated using (4) [22].

The contact mechanism between the ball and inner ring in ball bearing is a linear contact model that could be explained by using Hertzian theory. A linear contact model is only valid when the stress-strain relationship of the material is linear without exceeding the yield stress limit. Most of the contact cases were elasto-plastic contact which could not be explained by using Hertzian theory since the stress-strain relationship is not linear. The large plastic deformation, properties of viscoelastic, and time-dependent fatigue are examples of elasto-plastic contact behavior [23].

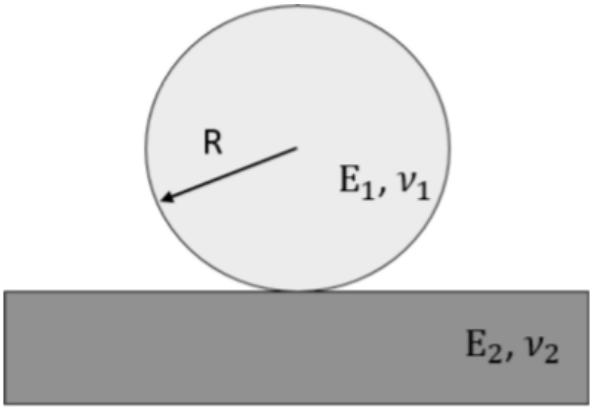

Fig. 1.A sphere loaded with force on a plate with different material properties [14].

III. FINITE ELEMENT ANALYSIS AND MODEL DESCRIPTION

A schematic diagram of the contact analysis is shown in Fig. 2. A boundary load, F was applied to the balls to obtain the stress distribution. An explicit finite element simulation was carried out to simulate the contact. The diameter of the ball was 12.7 mm while the length and width of the inner ring were 12 mm and 3 mm [13], [21]. A steel bearing with material properties of Young's modulus of 200 GPa, Poisson's ratio of 0.3, and density of 7.90 g/cm^3 was used [13]. There was a surface-to-surface interaction between the ball and the inner ring. The simulation time for the contact analysis was 0.13 s. The bottom of the inner ring was prevented from shifting in all directions, while the ball was constrained in the direction of the X-axis and the axis of rotation. A load was applied to the top of the ball bearing. The mesh of two-dimensional model is shown in Fig. 3. This model had an element number of 9522. A high element number was assigned to the contact area, namely at the centre of the ball and the inner ring, to save on the simulation time without affecting the accuracy of the simulation results, because the critical part in this simulation was the contact area between the ball and the inner ring [20]. Besides that, the element type of CPE4R, which is a plane strain element, was used.

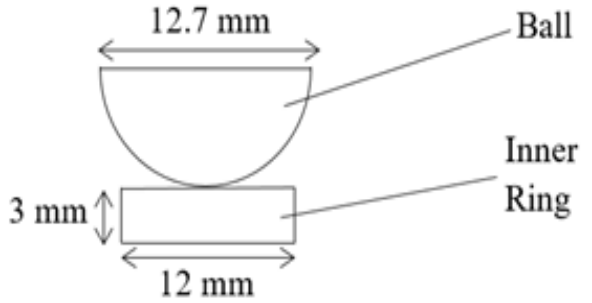

Fig. 2.Schematic diagram of contact analysis of ball bearing.

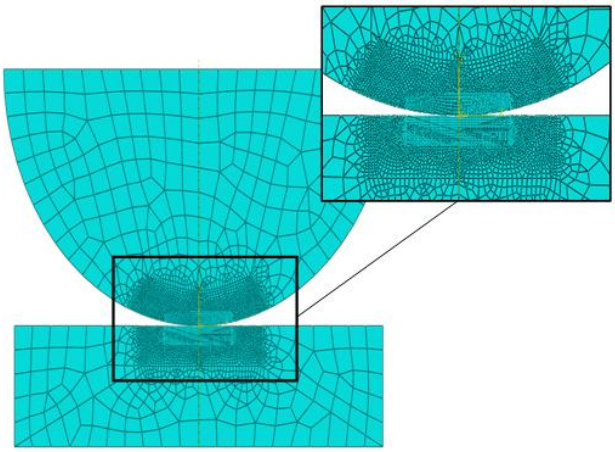

Fig. 3.Mesh for contact analysis.

IV. RESULT AND DISCUSSION

A. Model Verification

A convergence study was carried out on the finite element model. A mesh convergence study was performed to obtain more accurate results. The initial radius had an element number of 314, and the maximum contact pressure that was obtained from the simulation was 508 MPa when the applied load was 100 N. The finite element model started to have a consistent maximum contact pressure of 1750 MPa when the element number was 4340 as shown in Table I. The different meshes for diiferent element numbers are shown in Fig. 4. An amplitude of 55 was used to simulate the contact because this value, which was entered into the ABAQUS software, was able to reflect the actual case of what occurs to a ball bearing.

A maximum contact pressure of 1751 MPa was obtained by the simulation using the finite element method, while a value of 1784 MPa was obtained from other journals. In addition, a maximum contact pressure of 1800 MPa was obtained through analytical calculations that were carried out on this 2-dimensional model. There was a percentage difference of 1.90% between the results of the simulation and those of other journals, and a percentage difference of 2.72% between the results of the simulation and those obtained by analytical calculations. As the percentage differences were lower than 5%, it was confirmed that this model is accurate and can be used for various related studies. Table II shows a comparison of the simulation results and journal results. Fig. 5 shows the stress contours for the contact simulation with a boundary load of 100 N.

Table-I: Maximum contact pressure for different element number

Element Number	Maximum Contact Pressure (MPa)
314	508
362	1023
523	1166
728	1481
987	1836
1384	1748
4340	1750
9522 (mesh used)	1751
12652	1745
16214	1750
25258	1747

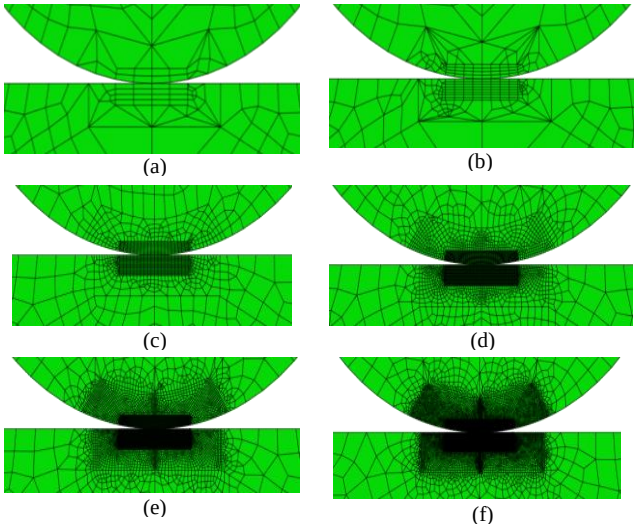

Fig. 4.Mesh of contact analysis for element number of 362 (a), 523 (b), 1384 (c), 4340 (d), 9522 (e), and 25258 (f).

Table-II: Results of simulation, validation journal and analytical calculation

Maximum contact pressure		
Model verification simulation	Validation simulations based on [13]	Result based analytical Calculations
1751 MPa	1785 MPa	1800 MPa
Percentage Difference	1.90 %	2.72 %

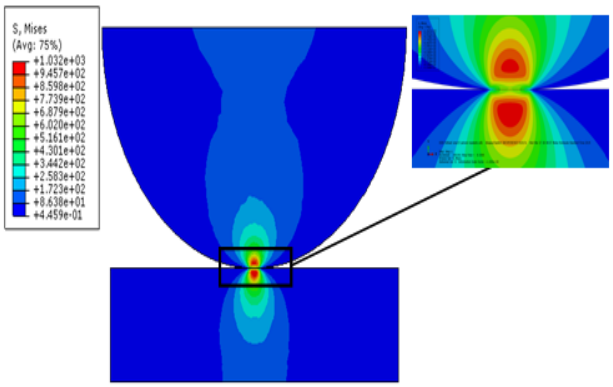

Fig. 5.Model verification result based stress contours for (load of 100 N).

B. Elastic Model: Contact Behavior on Ball Bearing

A variety of materials with different Young's modulus values were used for the elastic model for the contact analysis. Table III shows the properties of the materials used for the ball bearing. The inner ring material for this simulation was still maintained as steel, while three types of ball bearing materials were studied, namely steel, silicon nitride, and aluminium oxide. The contact simulation results using ball bearings made of the other materials are shown in Fig. 6. The maximum contact pressure for the simulation using ball bearings made of steel, silicon nitride and aluminium oxide was 1748 MPa, 1906 MPa, and 1970 MPa, respectively. The highest maximum contact pressure during the simulation was obtained when the ball bearing was made of aluminium oxide, which is a type of ceramic oxide with the highest Young's modulus of 380 GPa. Aluminium oxide is a very hard material compared to the other materials that were used. An explicit time step of 0.13 s was used for the contact simulation. The stress distribution for the contact simulation from time step 0 s to 0.13 s can be seen in Fig. 7. There was no stress distribution on the ball and inner ring of the ball bearing during time step 0 s as no boundary load was applied to the ball. The stress distribution started at 0.0065 s, and it increased over time as the boundary load increased. A boundary load of 100 N was applied to the ball at 0.13 s. The final shape of the stress distribution was obtained, as shown in Fig. 7. The highest von Mises stress was at the centre of the ball and inner ring of the ball bearing, but not at their surface. The stress distribution contours for the elastic deformation were elliptical in shape.

Table-III: Properties of ball bearing materials [16].

Ball material	E_1 (GPa)	Poisson's Ratio	Density (g/cm^3)
Steel bearing (GCr15)	200	0.3	7.90
Silicon nitride (Si_3N_4)	310	0.26	3.20
Aluminium oxide (Al_2O_3)	380	0.22	3.95

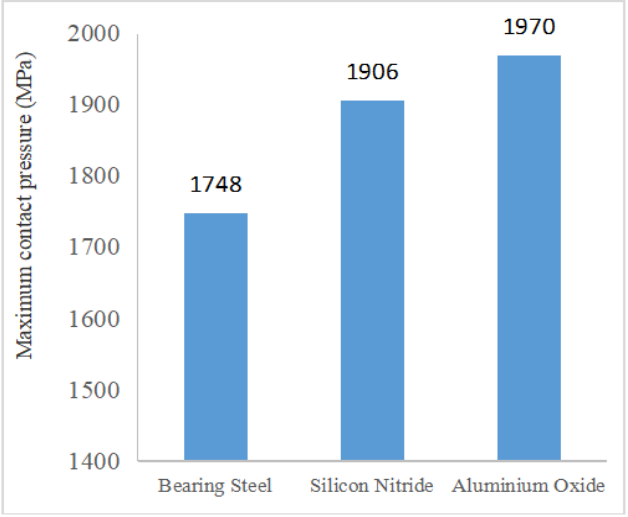

Fig. 6.Maximum contact pressure for 3 type materials

Time (s)	Stress distribution
0 $VM_{max100N}$ = 0 MPa	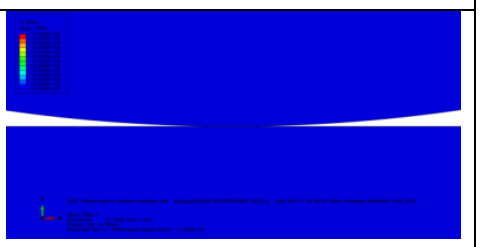
0.0325 $VM_{max100N}$ = 318 MPa	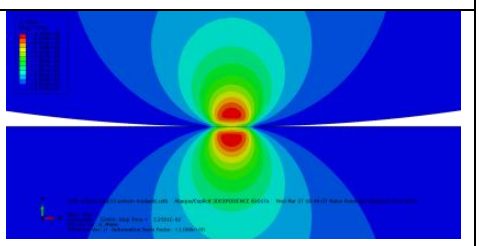
0.0650 $VM_{max100N}$ = 715 MPa	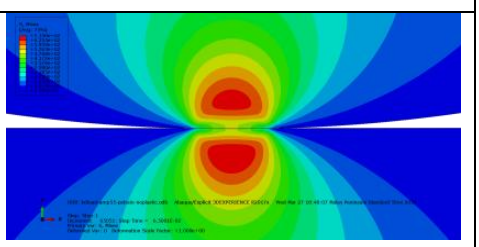
0.0975 $VM_{max100N}$ = 970 MPa	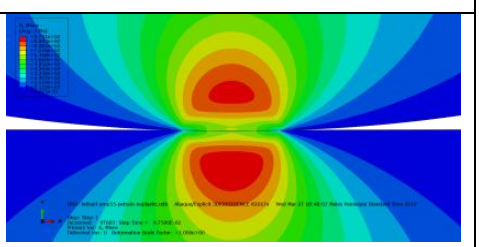

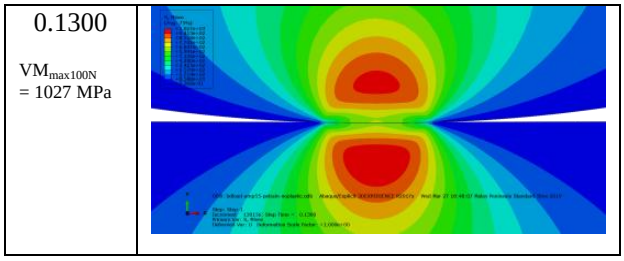

Fig. 7.Stress distribution for contact simulation from time step 0 s to 0.13 s.

C. Elastic-Plastic Model: Contact Behavior on Ball Bearing

In this section, the contact simulation using elastic-plastic model were performed to investigate the effect of stress distribution on three different types of materials. Based on the elastic-plastic model, the consideration has been taken in account on tangent modulus which is the slope between yield strength and ultimate strength. As a result the plasticity aspect that mimic the actual case can be determined accurately. In this case, the 100 N load was used as contact load on ball bearing. Yield strength and ultimate strength of the ball materials are shown in Table IV and these values were used in defining the plasticity of materials in ABAQUS.

The maximum contact pressures obtained through the simulations for ball materials of steel bearing, silicon nitride and aluminium oxide were 976 MPa, 1027 MPa, and 712 MPa. The Fig. 8 shows the maximum contact pressure for different types of ball materials while the Fig. 9 shows the stress contour of contact analysis for elasto-plastic deformation with load of 100 N. The maximum contact pressure obtained for bearing steel was lower than the maximum contact pressure for silicon nitride because the Young's modulus, yield strength and ultimate strength for silicon nitride is higher than bearing steel. The maximum contact pressure obtained for aluminium oxide material was lower than the maximum contact pressure of silicon nitride although the Young's modulus of silicon nitride is lower than Young's modulus of aluminium oxide because the yield strength and ultimate strength of aluminium oxide is much lower compared to silicon nitride. The higher yield strength and ultimate strength resulted in longer time for the material to yield. The material experienced a small increment of maximum contact pressure after the material started to yield. Ceramic bearing material has advantages like wear resistance, high temperature resistant, low density and high Young's modulus compared to bearing steel. Therefore, ceramic bearing is suitable to be used in conditions of high operating speed and temperature [16]. Fig. 10 shows the time step from 0 s to 0.13 s for contact simulation by using elasto-plastic model. An elliptical shape of stress contour can be observed during the time step of 0.0325 s. The maximum Von Mises stress happened at the region above and below the ball and inner ring. After time step of 0.0455 s, the material started to yield and the shape of stress contour was no longer an elliptical shape as shown in Fig. 10.

Table-IV:Yield strength and ultimate strength of ball material [3].

Material	Yield Strength (MPa)	Ultimate Strength (MPa)
Steel bearing (GCr15)	415	520
Silicon nitride (Si_3N_4)	524	690
Aluminium oxide (Al_2O_3)	200	300

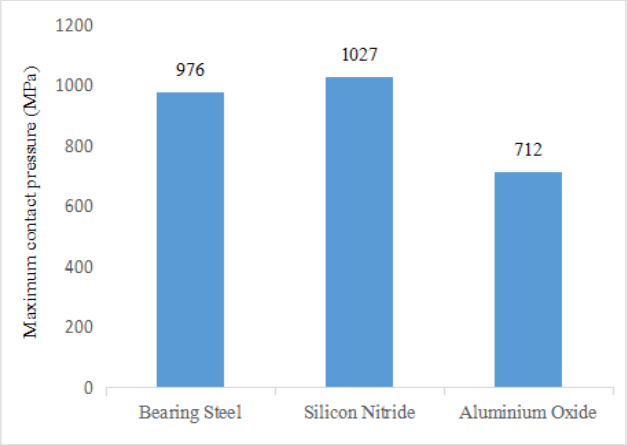

Fig. 8.Maximum contact pressure for steel bearing, silicon nitride and aluminium oxide.

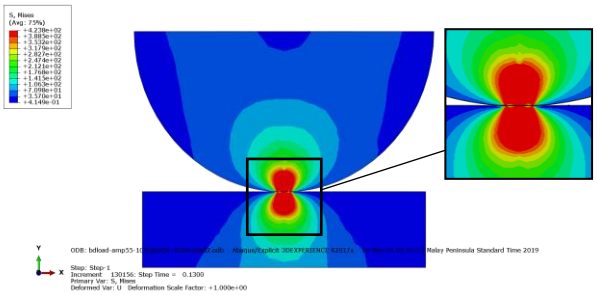

Fig. 9.Stress contours of contact analysis for elasto-plastic deformation with a boundary load of 100 N.

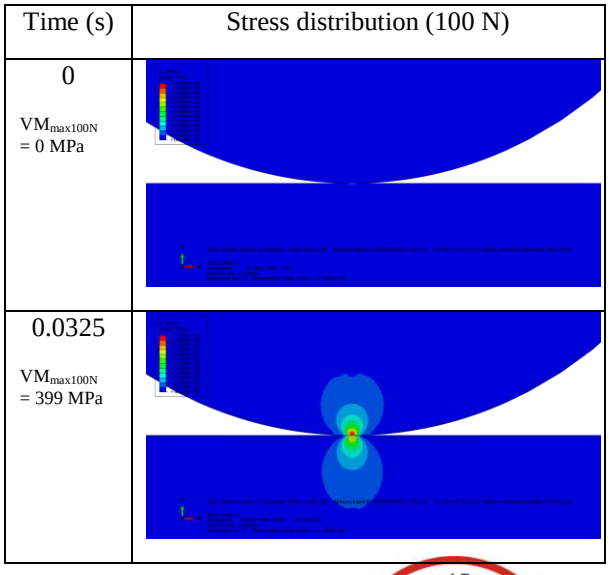

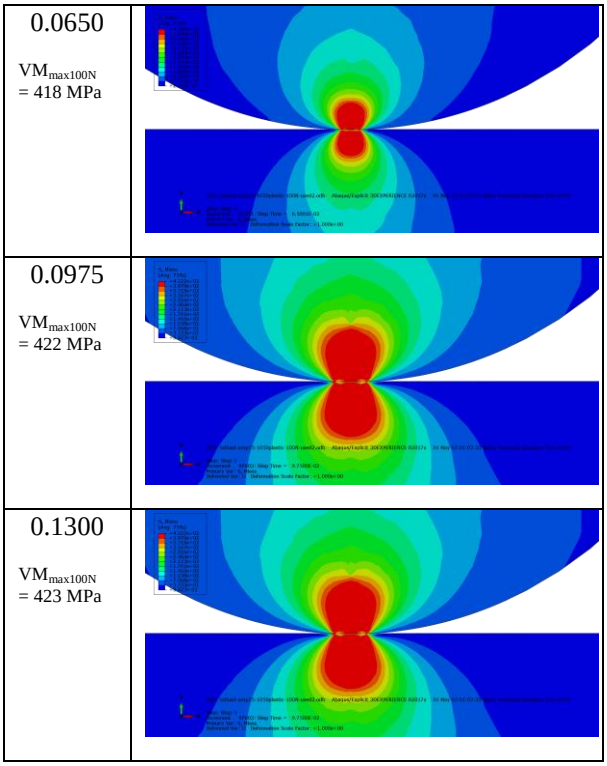

Fig. 10. Stress distribution from time step 0 s to 0.13 s for elastic-plastic contact model.

D. Comparison Maximum Contact Pressure on Different Types of Ball Bearing

The maximum contact pressure for contact simulation by using elastic model was higher compared to elasto-plastic model. The stress-strain relationship for elastic model material is linear with no proportional limit whereas stress-strain relationship for elasto-plastic model material is nonlinear. A higher maximum contact pressure for elastic model would be achieved since the material did not yield. A lower maximum contact pressure would be obtained for the elasto-plastic model because elasto-plastic material started to yield when stress was more the yield strength with small increment of maximum contact pressure. Therefore, the maximum contact pressure was lower when the plasticity is taken in account in simulating the contact of ball at inner ring. The elastic material would not experience yielding and the stress-strain relationship is linear whereas elasto-plastic material would yield after exceeding the yield strength with nonlinear stress-strain relationship. The maximum contact pressure would increase until the load was loaded completely for elastic model while maximum contact pressure would increase with little amount until the load was loaded completely for elasto-plastic model. The comparison between the maximum contact pressure of elastic model and elasto-plastic model is shown in Fig. 11. The stress distribution contour of the elastic model is elliptical shape through the whole simulation time. The maximum Von Mises stress was located at the region above and below the surface of ball and inner ring but not at the surface of the ball and inner ring. The elliptical shape of stress contour for elasto-plastic model still can be observed before the material started to yield like at time step of 0.0325 s as shown in Fig. 12. The stress contour became no longer elliptical shape after the material yielded. The maximum Von Mises stress happened near the contacting region of the ball and inner ring. The time step for contact simulation by using elastic model and elasto-plastic model is shown in Fig. 12.

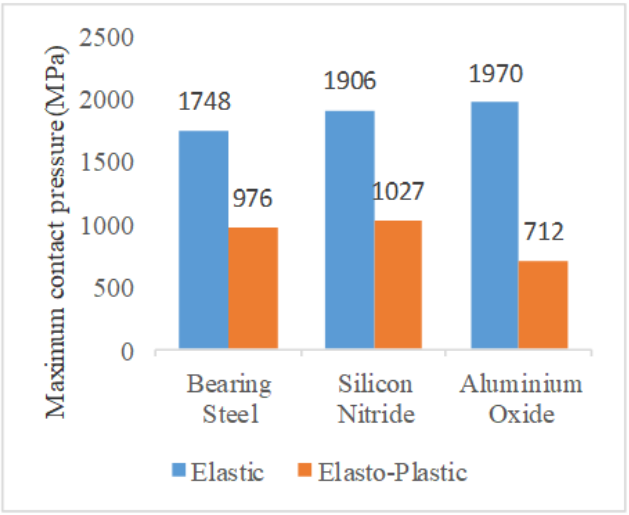

Fig. 11.Maximum contact pressure for different types of ball materials by using elastic model and elasto-plastic model.

Time (s)	Elastic Model	Elasto-Plastic Model
0 $VM_{max(elastic)}$ = 0 MPa $VM_{max(elasto-plastic)}$ = 0 MPa	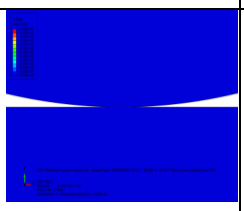	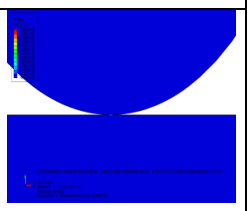
0.0325 $VM_{max(elastic)}$ = 318 MPa $VM_{max(elasto-plastic)}$ = 399 MPa	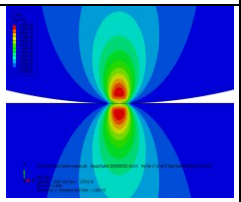	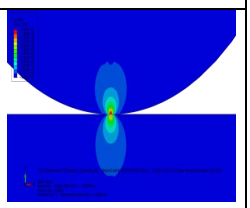
0.0650 $VM_{max(elastic)}$ = 715 MPa $VM_{max(elasto-plastic)}$ = 418 MPa	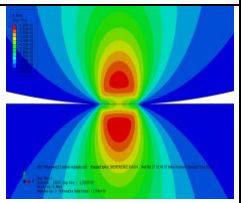	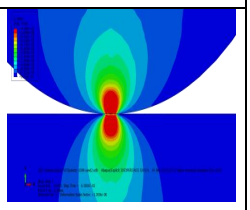
0.0975 $VM_{max(elastic)}$ = 970 MPa $VM_{max(elasto-plastic)}$ = 422 MPa	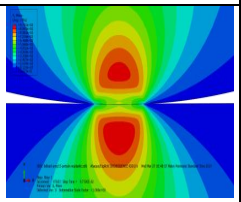	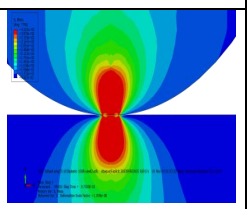

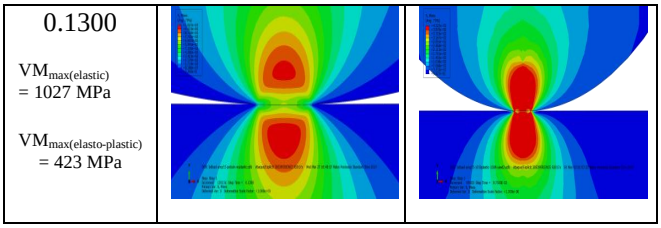

Fig. 12. Time steps for elastic and elasto-plastic contact model.

V. CONCLUSION

A contact analysis was conducted on a 6309 DGBB ball bearing using the finite element method. Several methods were used to verify the model that was used for the finite element simulations on the ball bearing. A mesh convergence was performed to ensure the accuracy of the results obtained from the simulations. Two models were establised to investigate the stress distribution and the effect of elastic and elasto-plastic deformation on the contact analysis of a ball bearing. An elastic model was used to examine the effect of using different materials for the balls in the ball bearing. For these simulations, steel, silicon nitride, and aluminium oxide were used as the material for the ball. The aluminium oxide ball was able to withstand the highest maximum contact pressure of 1970 MPa, followed by the silicon nitride and steel balls with values of 1906 MPa and 1748 MPa, respectively.

The maximum contact pressure obtained for ball material of bearing, silicon nitride and aluminium oxide by using elasto-plastic model were 976 MPa, 1027 MPa and 712 MPa. The highest maximum contact pressure obtained for the silicon nitride because silicon nitride has a higher yield strength and ultimate strength compared to the other materials of bearing steel and aluminium oxide. The higher yield strength and ultimate strength resulted in longer time for the material to yield. The material experienced a small increment of maximum contact pressure after the material started to yield. The maximum contact pressure obtained for material of bearing steel, silicon nitride and aluminium oxide by using elastic model was higher compared to elasto-plastic model. The elastic material would not experience yielding and the stress-strain relationship is linear. The maximum contact pressure would increase until the load was loaded completely. Elasto-plastic model considered the plasticity of material where the stress-strain relationship is nonlinear after exceeding the yield strength. The material started to yield when stress was more than the yield strength and maximum contact pressure would increase with little amount until the load was loaded completely.

ACKNOWLEDGEMENT

The authors would like to thank the Malaysia research foundation - Geran Universiti Penyelidikan: GUP-2018-149: and FRGS/1/2017/TK05/UKM/02/3 for funding this work.

REFERENCES

1. ABAQUS. 2017. Simulia user assistance 2017. United State: Dessault Systemes Simulia Corporation.
2. Arakere, N. K. 2016. Gigacycle rolling contact fatigue of bearing steels: A review. *International Journal of Fatigue* 93(June): 238–249.
3. Cambridge Engineering Selector software (CES EduPack 2019), 2019, Granta Design Limited, United Kingdom: Cambridge.
4. Ghezzi, I., Komba, E. W. H., Tonazzi, D., Bouscharain, N., Jenune, G. L., Coudert, J. B. & Massi, F. 2018. Damage evolution and contact surfaces analysis of high-loaded oscillating hybrid bearings. *Wear* 406: 1-12.
5. Gou, R., Zhang, X., Yang, W. & Chang, X. 2018. Finite element analysis of surface indentation on turbo-drill thrust ball bearing. *Australian Journal of Mechanical Engineering* 4846: 1–10.
6. Joshua, O.S., Babatunde, E.A. 2017. Predicting cashew nut cracking using hertz theory of contact stress. *Journal of the Saudi Society of Agricultural Sciences*, doi: http://dx.doi.org/10.1016/j.jssas.2017.04.002.
7. Kadam, S. B., Patil, P. G. & Patil, R. Y. 2018. Contact Stresses Analysis & Material Optimization Of Ball Bearing Using Hertz Contact Theory. *International Research Journal of Engineering and Technology (IRJET)* 5(1): 216-221.
8. Kenematsu, W. 2018. A review of rolling contact fatigue behavior of silicon nitride focusing on testing practices and crack propagation analysis. *Wear* 400: 10-20.
9. Koc, M. & Bozca, M. 2019. Finite Elements Method Modelling Of Rolling Bearings. *International Scientific Journal "Machines. Technologies. Materials"* 2: 62-65.
10. Kogut, L. & Etsion, L. 2002. Elastic-Plastic Contact Analysis of a Sphere and a Rigid Flat. Journal of Applied Mechanics 69: 657-662.
11. Zamri, W. F. H. W., Suang, N. J., Mohamed, I. F., Ariffin, A. K., & Din, M. F. M. 2019. Modelling of nanoindentation of TiALN and TiN thin film coatings for automotive bearing. International Journal of Recent Technology and Engineering, 8(3), 7194-7199..
12. Li, S. 2018. A mathematical model and numeric method for contact analysis of rolling bearings. *Mechanism and Machine Theory* 119: 61–73.
13. Londhe, N. D., Arakere, N. K. & Subhash, G. 2018. Extended Hertz Theory of Contact Mechanics for Case-Hardened Steels With Implications for Bearing Fatigue Life. *Journal of Tribology* 140(2): 1-11.
14. Mazgaonkar, N. & Stankovich, A. 2017. Fast Contact Method for Speeding up Solving of Finite Element Problems involving Non-Linear Contact Behavior. *SAE International*
15. Nazir, M. H, Khan, Z. A., Saeed, A. 2018. Experimental analysis and modelling of c-crack propagation in silicon nitride ball bearing element under rolling contact fatigue, *Tribology International*, doi: 10.1016/j.triboint.2018.04.030.
16. Qiu, M., Chen, L., Li, Y. & Yan, J. 2017. Bearing Tribology. 1st Ed. Beijing: Springer.
17. Raga, R., Khader, I., Chlup, Z. & Kailer, A. 2016, Damage initiation and evolution in silicon nitride under non-conforming lubricated hybrid rolling contact. *Wear* 360: 147-159.
18. Raju, D. V., Dixit, P., Rathore, N., Lakshmikant, P., Bubai, R. & Verma, R. 2018. Bearing Life Evaluation of Wheel Hub Ball Bearing Based on Finite Element Analysis. *Journal of Tribology* 140(1): 1-42.
19. Rezaei, A., Van Paepegem, W., De Baets, P., Ost, W. & Degrieck, J. 2012. Adaptive finite element simulation of wear evolution in radial sliding bearings. *Wear* 296(1–2): 660–671.
20. Siswanto, W. A., Surakarta, U. M. & Muniandy, N. 2015. Contact Pressure Prediction Comparison Using Implicit and Explicit Finite Element Methods and the Validation with Hertzian Theory. *International journal of mechanical & mechatronics engineering* 15(6): 1-8.
21. Zamri, W. F. H. W., Kosasih, B., Tieu, K., Ghopa, W. A. W., Din, M. F. M., Aziz, A. M., & Hassan, S. F. 2016. A simulation of friction behavior on oxidised high speed steel (HSS) work rolls. ARPN Journal of Engineering and Applied Sciences, 11(12), 7394-7400. Stachowiak, G. W. & Batchelor, A. W. 2005. Engineering tribology. 3rd Ed. Elsevier: United States.

22. Wakabayashi, N., Murakmi, N. & Takaichi, A. 2018. Current Applications of Finite Element Methods in Dentistry. *Handbook of Mechanics of Materials* 1-28.

AUTHORS PROFILE

Leong Chee Yau is a RA (research assistant) at Faculty of Engineering and Bulit Environment, UKM. He obtained his degree at Universiti Kebangsaan Malaysia (UKM). His research interests include, surface engineering, contact and wear modelling.

Wan Fathul Hakim W.Zamri is a senior lecturer at Universiti Kebangsaan Malaysia (UKM). He received his PhD in Mechanial Engineering at University of Wollongong (UoW), Australia. His areas of expertise include computational tribology and wear of materials.

Muhammad Faiz Md Din is a senior lecturer at Universiti Pertahanan Nasional Malaysia. He received his PhD at University of Wollongong (UoW), Australia. His expertise are superconductor, semiconductor, X-ray diffraction and neutron diffraction.

Intan Fadhlina Mohamed is a senior lecturer at Universiti Kebangsaan Malaysia (UKM). She received her PhD in Materials Engineering at KYUSHU University. Her areas of expertise are severe plastic deformation, nanostructured materials and precipitation hardening.

Azman Ahmad is a senior lecturer at University of Kuala Lumpur (MFI). He received his PhD in Mechanical Engineering at University of Wollongong (UoW), Australia. His areas of expertise include optimizatation, corrosion, and erosion.